

Di-boson and Tri-boson production at the LHC

Francisco Campanario*

Theory Division, IFIC, University of Valencia-CSIC, E-46980 Paterna, Valencia, Spain.

E-mail: francisco.campanario@ific.uv.es

Christoph Englert

SUPA, School of Physics and Astronomy, University of Glasgow, Glasgow, G12 8QQ, United Kingdom

E-mail: christoph.englert@glasgow.ac.uk

Michael Rauch

*Institut für Theoretische Physik, Universität Karlsruhe, KIT,
76128 Karlsruhe, Germany*

E-mail: michael.rauch@kit.edu

Sebastian Sapeta

*Institute for Particle Physics Phenomenology, Department of Physics, Durham University,
Durham, United Kingdom*

E-mail: sebastian.sapeta@durham.ac.uk

Dieter Zeppenfeld

*Institut für Theoretische Physik, Universität Karlsruhe, KIT,
76128 Karlsruhe, Germany*

E-mail: dieter.zeppenfeld@kit.edu

The status of di-boson and tri-boson production is shortly review. Using the VBFNLO and the LOOPSIM package, approximated results at NNLO QCD are given for WZ production. Results for $W^\pm\gamma\gamma + \text{jet}$ at NLO QCD are also shown.

*XXI International Workshop on Deep-Inelastic Scattering and Related Subject -DIS2013,
22-26 April 2013
Marseilles,France*

*Speaker.

1. Introduction

Di-boson and tri-boson production processes provide a rich source of information at hadron colliders and have been already intensively studied both from the theoretical and the experimental side. They are important backgrounds to both Standard Model (SM) and beyond standard model (BSM) searches. As a signal, they yield information on triple and quartic gauge couplings.

In this proceedings article, a short overview of the theoretical status of di-boson production and recent results beyond NLO QCD for WZ production will be presented in Section 2. A brief overview of tri-boson production and results for $W\gamma\gamma + jet$ will be given in Section 3

2. Di-boson Production

NLO QCD corrections for di-boson production at hadron colliders were computed in Refs. [1]. The size of these corrections, for inclusive cuts, ranges in the order of the 40% to 100%. The big impact of the NLO corrections is mainly due to the appearance of new sub-processes at this order as part of the real corrections, namely, gluon initiated processes. These are enhanced at the LHC due to the large gluonic pdfs and partially compensate the suppression on α_s .

For example, for WZ production (see Fig. 1), at LO only the $q\bar{q} \rightarrow WZ$ production mode contributes, however, at NLO, new $gq (g\bar{q}) \rightarrow WZq (\bar{q})$ channel, with enhanced luminosity, appears. The corrections for $W\gamma$ production can be even larger due to a radiation zero [2] which suppresses the LO contributions. Gluonic neutral radiation as part of the real corrections breaks down the radiation pattern resulting in large NLO corrections.

The NLO differential distributions are sizable and phase space dependent – therefore normalizing the LO differential distributions by the K-factor (NLO/LO) of the integrated cross section does not provide reliable predictions. Giant K-factors of order 20 for commonly used observables can appear, which have a topological phase space origin. At LO, e.g. for WZ see Fig. 1 (left), only back-to-back WZ configurations are possible whereas at NLO, one electroweak boson can recoil against one parton and the other can be emitted arbitrarily soft or collinear, yielding large logarithmic enhancements.

Gluon-gluon-initiated contributions for neutral production processes with a closed fermion loop, which are formally at QCD NNLO due to their one-loop \times one-loop nature, have also been computed in Refs. [3]. The corrections can be as large as 20%, the α_s^2 suppression is compensated partially by the large gluonic pdfs.

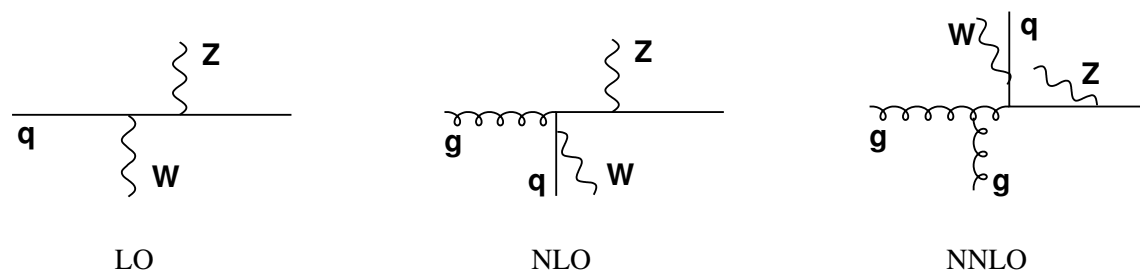


Figure 1: Example diagram contributing to WZ production at LO, NLO and NNLO.

The QCD NLO corrections for all production modes, and also the NNLO QCD fermion-loop gluon initiated contributions for neutral production channels, are available in the latest release of the VBFNLO package [4], which includes also anomalous coupling effects at NLO.

Recently, EW corrections for almost all diboson production processes have been computed in Refs. [5] for on-shell production. The corrections can be sizable in the tails of the differential distributions for commonly used experimental analyses.

Because the NLO QCD corrections turn out to be extremely large, it is important to assess the size of the NNLO QCD corrections. At this order, as can be seen in Fig. 1 for the WZ case, new topologies and sub-processes appear first at NNLO, which can result in large corrections.

The full NNLO corrections for di-photon production have been provided in Ref. [6] and turned out to be sizable. The two-loop virtual corrections for di-boson on-shell production have been presented in Refs. [7]. Results for $VV + jet$ at NLO QCD, which provide the one-loop real-virtual and double real corrections have been also computed in a series of papers [8, 9] and are available either in VBFNLO [4] or in MCFM [10].

Given the fact that $VV + jet$ at NLO QCD provides an essential piece of the NNLO QCD corrections of VV production, accounting both for the new sub-processes and topologies appearing first at NNLO, the question is whether we can use this information to provide approximate results at NNLO for VV production. We used the LOOPSIM method [11] to accomplish this and compute approximate NNLO QCD corrections for WZ production. The LOOPSIM method is based on unitarity and is able to merge processes with different jet multiplicities in a consistent way. To produce approximate NNLO results for WZ production (\bar{n} NLO in LOOPSIM notation), the program needs to merge samples of WZ and WZj at NLO accuracy. The WZj samples at NLO, computed in Ref. [9], are obtained from the VBFNLO package, which also provides the WZ events at NLO. An interface was created to communicate between the two programs for this purpose [12]. From the tree level and the one-loop correction events of WZj , LOOPSIM produces approximated 2-loop virtual counterterms for WZ production, which are designed to cancel the infrared divergences. The LOOPSIM method has an internal parameter, R_{LS} , to evaluate the uncertainty. It will be shown that this is smaller than the remaining factorization and renormalization scale uncertainties.

In the following, results at \bar{n} NLO are given. They were studied in Ref. [12]. The cuts applied were defined to closely follow the experimental analyses,

$$p_{T,\ell} \geq 15(20), \quad |y_\ell| \leq 2.5, \quad E_{T,\text{miss}} > 30 \text{ GeV}, \quad 60 < m_{l+l^-} < 120 \text{ GeV}, \quad (2.1)$$

where the parenthesis indicates cuts applied to leptons coming from Z. For observables that involve jets, we consider only those jets that lie in the rapidity range $|y_{\text{jet}}| \leq 4.5$ and have transverse momenta $p_{T,\text{jet}} \geq 30 \text{ GeV}$. The anti- k_t algorithm [14] has been used, as implemented in FastJet [15], with the radius $R = 0.45$. Additionally, the leptons and jets are required to be well separated $\Delta R_{l(l,j)} > 0.3$. For the central value of the renormalization and factorization scale we use

$$\mu_0 = \mu_R = \mu_F = (\sum p_{T,\text{partons}} + \sqrt{p_{T,W}^2 + M_W^2} + \sqrt{p_{T,Z}^2 + M_Z^2})/2.$$

As a first check of our setup, we have merged $WZ@LO$ and $WZj@LO$ to produce $WZ@\bar{n}LO$, which can be tested against the full $WZ@NLO$ result. In the left panel of Fig. 2, we show the effective mass defined by

$$H_T = \sum p_{T,\text{jets}} + \sum p_{T,l} + E_{T,\text{miss}}. \quad (2.2)$$

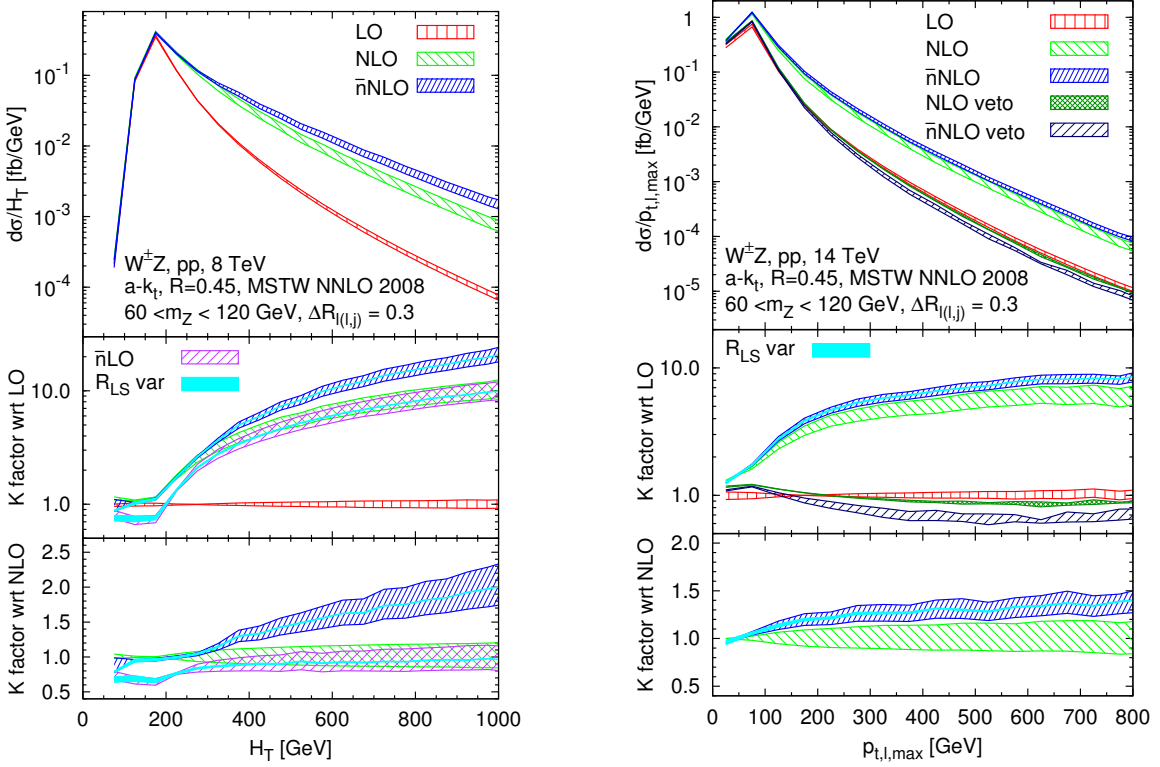


Figure 2: Differential cross sections and K factors for the effective mass observable, defined in Eq. (2.2), for the LHC at $\sqrt{s} = 8$ TeV (left). Differential cross sections and K factors for the p_T of the hardest lepton for the LHC at $\sqrt{s} = 14$ TeV (right). The bands correspond to varying $\mu_F = \mu_R$ by factors 1/2 and 2 around the central value. The cyan solid bands give the uncertainty related to the R_{LS} parameter varied between 0.5 and 1.5. The distribution are sums of contributions from two unlike flavor decay channels, $ee\mu\nu_\mu$ and $\mu\mu e\nu_e$.

One can observe in the central panel that the \bar{n} LO result converges to the full NLO result quickly, predicting correctly K-factors of order 10. The \bar{n} NLO corrections can be as large as 100% compared to NLO (bottom panel of Fig. 2) and they are clearly beyond the NLO scale uncertainties. The R_{LS} uncertainties are small in comparison to those from varying the factorization and renormalization scales, which show a marginal reduction. The latter is related to the fact that the H_T observable favours regions of phase space associated with new topologies entering first at NNLO, which are computed only at LO.

In the right panel of Fig. 2, we present results for the differential distribution of the lepton with higher transverse momenta. One observes that the \bar{n} NLO corrections are large and beyond the scale uncertainty, reaching values as high as 40%. The scale uncertainty is significantly improved and the R_{LS} uncertainty is marginal. We include the vetoed sample to mimic some of the experimental analyses. One can see that the \bar{n} NLO corrections are negative and exhibit larger scale uncertainties than the NLO corrections, showing the known feature of an artificially small scale uncertainty of NLO predictions with jet veto.

3. Tri-boson production

Tri-boson production processes are important backgrounds to SM and BSM searches. They have been already examined in many experimental analyses. As a signal, they allow us to quantify possible deviations from the Standard Model coming from anomalous triple and quartic gauge couplings. From the theoretical side, all the possible production modes have been computed at NLO QCD within the VBFNLO collaboration in Refs. [16, 17], including the leptonic decays of the vector bosons and all off-shell effects. Some of the channels have been computed by other groups Refs. [18, 19] for on-shell production and neglecting Higgs boson exchange. The NLO QCD corrections are large ranging from 40%- 100% at the cross section level and even larger for differential distributions. The origin of the size of the corrections is the same as for the di-boson case. At NLO, new sub-processes and topologies appear.

$W^\pm\gamma\gamma$ production is the tri-boson production channel with the largest K-factor for the integrated cross section (~ 3) for standard experimental inclusive cuts. This feature, similarly to the $W\gamma$ case, is due to the radiation zero [2] pattern present at LO and broken at NLO by additional real QCD radiation, $W^\pm\gamma\gamma$ +jet, as part of the NLO contributions. In Ref [17, 19], it was shown that an additional jet veto-cut might help in the detection of the radiation zero. However, due to the aforementioned problem with the exclusive vetoed samples, this procedure raises the question of the reliability of the predictions. Additionally, the remaining scale uncertainties at NLO QCD are due to unbalanced gluon-induced real radiation computed at LO, e.g., $gq \rightarrow W^\pm\gamma\gamma q$. Thus, to realistically assess the uncertainties, also concerning anomalous coupling searches and as an important step towards a NNLO QCD or a LOOPSIM \bar{n} NLO QCD calculation of $W^\pm\gamma\gamma$, we calculated $W^\pm\gamma\gamma$ +jet at NLO QCD.

$W^\pm\gamma\gamma$ + jet at NLO QCD includes the evaluation of the complex hexagon virtual amplitudes computed in Ref. [20]. These pose a challenge not only at the level of the analytical calculation, but also concerning the CPU time required to perform a full $2 \rightarrow 4$ process at NLO QCD.

The details on the setup can be found in Ref. [21]. We consider W^\pm decays to the first two lepton generations, i.e, $W \rightarrow e\nu_e(+\gamma), \mu\nu_\mu(+\gamma)$. Both contributions are summed in Fig 3.

K-factors of about 1.4, which are similar to the ones found in other multi-boson+jet processes [8, 9] are found for the LHC at $\sqrt{s} = 14$ TeV. This moderate K-factor as compared to corrections of $\sim 300\%$ for $W^\pm\gamma\gamma$ production confirms that the large integrated K-factor encountered in $W^\pm\gamma\gamma$ production can mainly be attributed to radiation zero cancellations, which are not present in $W^\pm\gamma\gamma$ + jet. The scale dependence of the $W\gamma\gamma j$ production cross section turns out to be modest at about 10%. The phase space dependence of the QCD corrections is non-trivial and sizable. Additional parton emission modifies the transverse momentum and invariant mass spectra. The leading jet becomes slightly harder at NLO as can be inferred from the differential K factor in the bottom panel of Fig. 3. Vetoed real-emission distributions are plagued with large uncertainties (Fig. 3, left).

4. Summary

Results beyond NLO QCD have been presented for WZ production at the LHC as well as for $W^\pm\gamma\gamma$ + jet at NLO. The corrections are beyond scale uncertainties and exhibit a non-trivial phase

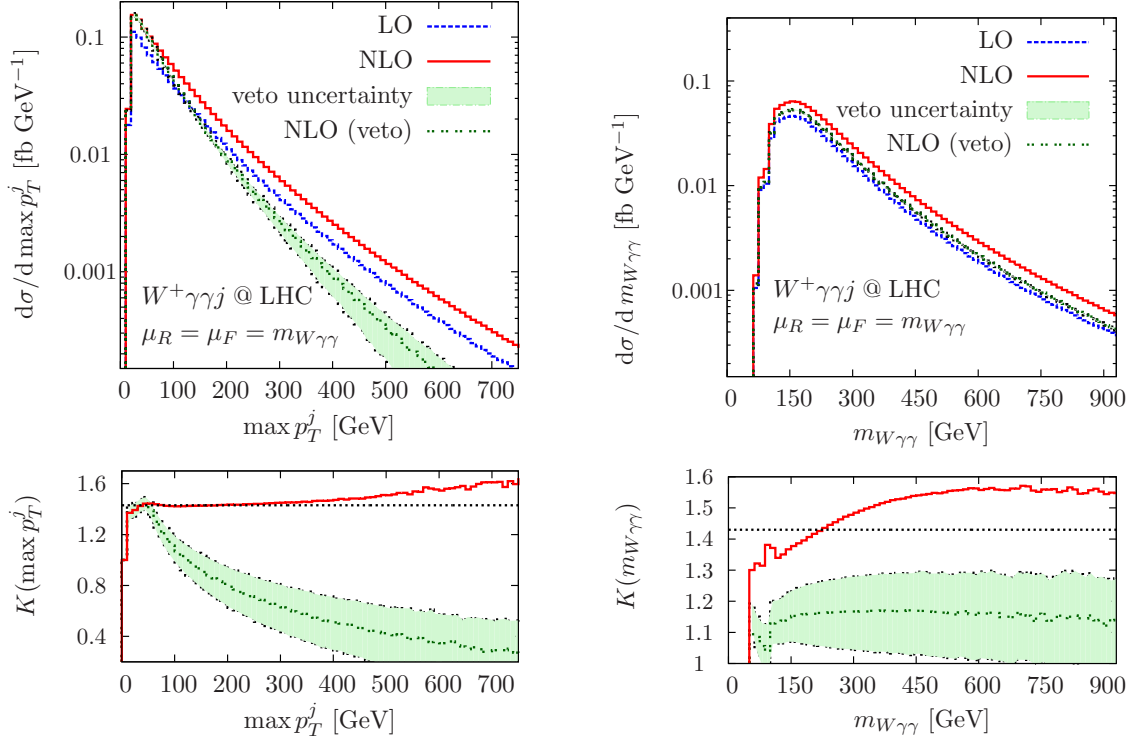


Figure 3: Differential $\max p_T^j$ and $m_{W\gamma\gamma}$ distribution for inclusive and exclusive $l^+\bar{\nu}\gamma\gamma$ +jet production.

space dependence. When comparing precisely measured distributions in these channels against Monte Carlo predictions, un-included QCD corrections could be misinterpreted for anomalous electroweak trilinear or quartic couplings arising from new interactions beyond the SM.

Acknowledgments

We acknowledge support by the Deutsche Forschungsgemeinschaft under SFB TR-9 “Compuergestützte Theoretische Teilchenphysik”. FC is funded by a Marie Curie fellowship (PIEFGA-2011-298960) and partially by MINECO (FPA2011-23596) and by LHCPHENONET (PITN-GA-2010-264564). MR acknowledges support by the Initiative and Networking Fund of the Helmholtz Association, contract HA-101(“Physics at the Terascale”). SS was in part supported by European Commission under contract PITN-GA-2010-264564.

References

- [1] J. Ohnemus, *Phys.Rev.* **D47** (1993) 940–955. U. Baur, T. Han, and J. Ohnemus, *Phys.Rev.* **D57** (1998) 2823–2836. L. J. Dixon, Z. Kunszt, and A. Signer, *Nucl.Phys.* **B531** (1998) 3–23. L. J. Dixon, Z. Kunszt, and A. Signer, *Phys.Rev.* **D60** (1999) 114037.
- [2] R. W. Brown, K. L. Kowalski, S. J. Brodsky, *Phys. Rev.* **D28** (1983) 624.
- [3] D. A. Dicus and S. S. D. Willenbrock, *Phys. Rev. D* **37** (1988) 1801. L. Ametller, E. Gava, N. Paver and D. Treleani, *Phys. Rev.* **D32** (1985) 1699. J. J. van der Bij and E. W. N. Glover, *Phys. Lett.* **B206**

- (1988) 701. K. Adamson, D. de Florian and A. Signer, *Phys.Rev.* **D67** (2003). 034016. D. A. Dicus, C. Kao and W. Repko, *Phys.Rev.* **D36** (1987) 1570. E. Glover and J. van der Bij, *Phys.Lett.* **B219** (1989) 488. E. W. N. Glover and J. J. van der Bij, *Nucl. Phys.* **B321** (1989) 561. T. Binoth, N. Kauer and P. Mertsch, [0807.0024](#). T. Binoth, M. Ciccolini, N. Kauer and M. Kramer, *JHEP* **03** (2005). T. Binoth, M. Ciccolini, N. Kauer and M. Kramer, *JHEP* **12** (2006) 046.
- [4] K. Arnold *et al.*, *Comput. Phys. Commun.* **180** (2009) 1661; arXiv:1107.4038 ;arXiv:1207.4975.
- [5] E. Accomando and A. Kaiser, *Phys.Rev.* **D73** (2006) 093006. E. Accomando, A. Denner, and A. Kaiser, *Nucl.Phys.* **B706** (2005) 325–371. E. Accomando, A. Denner, and C. Meier, *Eur.Phys.J.* **C47** (2006) 125–146. A. Bierweiler, T. Kasprzik, and J. H. Kühn, arXiv:1305.5402.
- [6] S. Catani, L. Cieri, D. de Florian, G. Ferrera, and M. Grazzini, *Phys.Rev.Lett.* **108** (2012) 072001.
- [7] Z. Bern, A. De Freitas, and L. J. Dixon, *JHEP* **0109** (2001) 037. T. Gehrmann and L. Tancredi, *JHEP* **1202** (2012) 004. T. Gehrmann, L. Tancredi, and E. Weihs, *JHEP* **1304** (2013) 101. G. Chachamis, M. Czakon, and D. Eiras, *JHEP* **0812** (2008) 003. T. Gehrmann, L. Tancredi and E. Weihs, arXiv:1306.6344.
- [8] V. Del Duca, F. Maltoni, Z. Nagy and Z. Trocsanyi, *JHEP* **0304** (2003) 059. S. Dittmaier, S. Kallweit and P. Uwer, *Phys. Rev. Lett.* **100**, 062003 (2008); *Nucl. Phys. B* **826** (2010) 18. T. Binoth, T. Gleisberg, S. Karg, N. Kauer and G. Sanguinetti, *Phys. Lett. B* **683**, 154 (2010). F. Campanario, C. Englert, M. Spannowsky and D. Zeppenfeld, *Europhys. Lett.* **88** (2009) 11001. F. Campanario, C. Englert and M. Spannowsky, *Phys. Rev. D* **83** (2011) 074009. F. Campanario, C. Englert and M. Spannowsky, *Phys. Rev. D* **82** (2010) 054015. J. M. Campbell, H. B. Hartanto and C. Williams, *JHEP* **1211** (2012) 162.
- [9] F. Campanario, C. Englert, S. Kallweit, M. Spannowsky and D. Zeppenfeld, *JHEP* **1007** (2010) 076.
- [10] J. M. Campbell and R. K. Ellis, *Nucl. Phys. Proc. Suppl.* **205-206** (2010) 10.
- [11] M. Rubin, G. P. Salam and S. Sapeta, *JHEP* **1009** (2010) 084.
- [12] F. Campanario and S. Sapeta, *Phys. Lett. B* **718** (2012) 100.
- [13] A. D. Martin, W. J. Stirling, R. S. Thorne and G. Watt, *Eur. Phys. J. C* **63** (2009) 189.
- [14] M. Cacciari, G. P. Salam and G. Soyez, *JHEP* **0804** (2008) 063.
- [15] M. Cacciari and G. P. Salam, *Phys. Lett. B* **641** (2006) 57. M. Cacciari, G. P. Salam and G. Soyez, <http://fastjet.fr/>.
- [16] V. Hankele and D. Zeppenfeld, *Phys. Lett. B* **661** (2008) 103. F. Campanario, V. Hankele, C. Oleari, S. Prestel and D. Zeppenfeld, *Phys. Rev. D* **78** (2008) 094012. G. Bozzi, F. Campanario, V. Hankele and D. Zeppenfeld, *Phys. Rev. D* **81** (2010) 094030. G. Bozzi, F. Campanario, M. Rauch, H. Rzehak and D. Zeppenfeld, *Phys. Lett. B* **696**, 4 (2011). G. Bozzi, F. Campanario, M. Rauch and D. Zeppenfeld, *Phys. Rev. D* **84** (2011) 074028.
- [17] G. Bozzi, F. Campanario, M. Rauch and D. Zeppenfeld, *Phys. Rev. D* **83** (2011) 114035.
- [18] A. Lazopoulos, K. Melnikov and F. Petriello, *Phys. Rev. D* **76** (2007) 014001. T. Binoth, G. Ossola, C. G. Papadopoulos and R. Pittau, *JHEP* **0806** (2008) 082,
- [19] U. Baur, D. Wackerroth and M. M. Weber, *PoS RADCOR2009*, 067 (2010), arXiv:1001.2688.
- [20] F. Campanario, *JHEP* **1110** (2011) 070.
- [21] F. Campanario, C. Englert, M. Rauch and D. Zeppenfeld, *Phys. Lett. B* **704** (2011) 515.